



UNIVERSITY OF NIŠ

The scientific journal FACTA UNIVERSITATIS

Series: **Mechanics, Automatic Control and Robotics** Vol.2, No 8, 1998 pp. 655 - 668

Editor of series: Katica (Stevanovi) Hedrih, e-mail: katica@masfak.masfak.ni.ac.yu

Address: Univerzitetski trg 2, 18000 Niš, YU, Tel: (018) 547-095, Fax: (018)-547-950

<http://ni.ac.yu/Facta>

## VELOCITY CORRELATIONS IN THE WAKE BEHIND A CYLINDER

UDC: 532.517.4

Dragan V. Petrović<sup>1</sup>, Thoralf C. Schenck<sup>2</sup>, Franz Durst<sup>2</sup>

<sup>1</sup>Faculty of Agriculture, Institute for Agricultural Mechanization,  
Chair for Mathematics and Physics, University of Belgrade

<sup>2</sup>Lehrstuhl für Stromungsmechanik – LSTM, Technische Fakultät  
Friedrich-Alexander Universität Erlangen-Nürnberg

**Abstract.** *In the paper is verified the existence of statistical relationships between higher-order velocity moments in the plain wake behind a cylinder. Although some differences are present, these connections are analogue to the general trends previously noticed in turbulent boundary layer and free jet:  $SS_{U,V}=10*S_{U,V}$ ,  $SF_{U,V}=15*F_{U,V}-30$ ,  $F_U=1.62*S_U^2+2.65$  and  $F_V=3.13*S_V^2+3.48$ . They represent a good base for further statistical analysis of turbulent flows and resolving the closure problem.*

### 1. INTRODUCTION

Although turbulence is the very old problem of fluid mechanics, it is still unresolved. This phenomenon is generally present in most applications related to energy conversion, flow problems, transport systems, etc. The objectives of current studies are mostly concentrated to understanding the physical mechanisms of turbulence and to deriving theoretical and experimental tools for predicting and controlling these flows. Possible way to describe turbulence originates from the general laws of continuum mechanics, established by Reynolds at the end of the last century. It assumes decomposition of turbulent velocity field in the two fields, which correspond to a mean motion and time-dependent fluctuations of fluid velocity. Unfortunately, non-linearity of basic hydrodynamic equations causes the resulting system of time-averaged equations to be unclosed. This is the first, among many other reasons, why researches are currently mostly occupied by turbulence closure problem for the mean quantities.

Various theoretical approaches, for closing the system of equations mentioned above, have been suggested. Statistical description of turbulence, based on Hopf's equation [13], formally provides the analytical solution for the closure problem. This equation is closed and linear, providing virtually a complete statistical description of turbulence. But, from

the practical point of view, big mathematical difficulties arise. Current belief is that there is no way for success, if this equation is used.

Researches in the contemporary fluid mechanics ([4] for example) mainly believe that the most promising approach for providing the turbulence closure should be based on the equations for the moments of turbulence quantities. These ideas mostly originate from *Chou 1945*, who formulated the approach for closing the dynamic equations of moments using the two-point correlation technique. Closing the system of time averaged equations suffers from the lack of suitable data for validating the closure assumptions. Measurement of almost all quantities, required by the applied closure hypothesis, is very complicated and sometimes nearly impossible. Fortunately, direct numerical simulation enabled significant progress in this area of turbulence research, providing suitable numerical database [12]. This is one of the main reasons, why turbulence researches closely follows development of digital computer technology.

Usual practice is to analyze turbulence as a stochastic phenomenon. Therefore, the highest reliability in its describing corresponds to the theories based on the statistical assumptions joined to the dynamic equations of fluid flow. Statistical approach requires information about the evolution of the probability-density distributions and corresponding correlation functions. Increased order of the correlation functions improves the universality of the certain statistical turbulent model.

## 2. MOTIVATION FOR THE WORK

The idea for this work was found in the few papers, but mostly in [4]. These authors presented a statistical approach for predicting turbulent flows, based on the system of dynamic equations of arbitrary order for the higher-order moments of turbulent velocity distributions. Specifically, they analyzed turbulent boundary layer. General form of this system can be derived starting from the Navier-Stokes and continuity equation. Splitting the instantaneous velocity and pressure in the mean and fluctuating components (according to Reynolds) gives the following expressions for instantaneous fluctuations:

$$\frac{\partial u_j}{\partial t} + U_i \frac{\partial u_j}{\partial x_i} + u_i \frac{\partial U_j}{\partial x_i} + \frac{\partial}{\partial x_i} (u_i u_j - \overline{u_i u_j}) = -\frac{1}{\rho} \frac{\partial p}{\partial x_j} + \nu \frac{\partial^2 u_j}{\partial x_i \partial x_i} \quad (1)$$

$$\frac{\partial u_i}{\partial x_i} = 0 \quad (2)$$

In the equation (1) and (2), the summation convention is applied over all double indices.

After multiplication of (1) by  $\mathbf{u}_j^n$  and utilization of equation (2), the following general system of equations that governs both normal and mixed higher-order moments arise:

$$\begin{aligned} & \frac{1}{1+n} \frac{\partial \overline{u_j^{n+1}}}{\partial t} + \frac{U_i}{n+1} \frac{\partial \overline{u_j^{n+1}}}{\partial x_i} + \overline{u_j^n u_i} \frac{\partial U_j}{\partial x_i} + \\ & + \frac{1}{1+n} \frac{\partial \overline{u_j^{n+1} u_i}}{\partial x_i} - \overline{u_j^n} \frac{\partial \overline{u_i u_j}}{\partial x_i} = \overline{u_j^n \Omega_j} \end{aligned} \quad (3)$$

In the previous expressions, turbulence parameter:

$$\Omega_j = -\frac{1}{\rho} \frac{\partial p}{\partial x_j} + \nu \frac{\partial^2 u_j}{\partial x_i \partial x_i} \quad (4)$$

is a function of space and time. It should be noted that the summation convention does not hold for repeated index  $j$  in (3). System of equations (3) is fairly complex. Fortunately, they can be simplified for any certain flow configuration. *Durst and Jovanović* [4] analyzed boundary layer flow, starting from the following expressions for the central moments:

$$\overline{u_j^n u_2} \frac{dU_1}{dx_2} \delta_{1j} + \frac{1}{1+n} \frac{d\overline{u_j^{n+1} u_2}}{dx_2} - \overline{u_j^n} \frac{d\overline{u_j u_2}}{dx_2} = \overline{u_j^n \Omega_j} \quad (5)$$

Although system of equations (5) is developed primarily for steady channel flow, they claimed that it is also a very good approximation for wall bounded flow.

Since system (5) contains the terms based on two types of correlation, namely  $\overline{u_j^n u_2}$  and  $\overline{u_j^n \Omega_j}$ , it is suitable for further statistical consideration to introduce the three-dimensional joint probability density distribution:

$$P_j(u_j, u_2, \Omega_j), \dots, j = 1, 2, 3. \quad (6)$$

and its marginal distributions:

$$P^{j(1)}(u_j, u_2) = \int_{-\infty}^{\infty} P^j(u_j, u_2, \Omega_j) d\Omega_j \quad (7)$$

$$P^{j(2)}(u_j, \Omega_j) = \int_{-\infty}^{\infty} P^j(u_j, u_2, \Omega_j) du_2 \quad (8)$$

However, introducing (7) and (8) generates a new problem: their exact analytical forms are unknown. One way to resolve it is to expand (7) and (8) in terms of higher-order cumulants. Truncation of these expansions enables prediction of the next few succeeding higher-order correlations as functions of lower order correlations. Substitution of predicted correlations in the derived dynamic equation for higher-order moments provide the possibility to eliminate the compound correlations  $\overline{u_j^n \Omega_j}$  from the right-hand side of equation (5) and formulate an alternative set of equations for the moments, which contains only velocity correlations. Resulting system of equations represent the suitable basis for further statistical analysis of turbulence and resolving the closure problem.

### 3. PREVIOUS RESULTS

We were encouraged to prepare this work after analyzing available results of other researches. Comprehensive review of statistical relationships between higher-order velocity moments in the channel flow, boundary layer and free jet can be found in [4]. They combined own experimental data with corresponding results of many other

researches and reported the following relationships between skewness **S** and flatness **F** factors:

$$F_U \approx 2.65 + 1.62S_U^2, \quad F_V \approx 3.13 + 2.48S_V^2 \quad (9-10)$$

for the longitudinal **U** and transversal **V** velocity component, where:

$$S_j = \overline{u_j^3} / \sigma_j^3, \quad F_j = \overline{u_j^4} / \sigma_j^4, \quad \sigma_j = \sqrt{\overline{u_j^2}}, \quad (U: j = 1; \quad V: j = 2) \quad (11-13)$$

Besides relationships (9) and (10) for successive-order moments, in the boundary layer are also evidenced linear connections between even and odd central moments [6]. Their functional shapes are equal for both **U** and **V** component. Among many other available expressions, formulated by truncating the Gram-Charlier series expansions, we analyzed the following two relationships:

$$SS \approx 10S, \quad SF \approx 15F - 30 \quad (14-15)$$

where:

$$SS_j = \overline{u_j^5} / \sigma_j^5, \quad SF_j = \overline{u_j^6} / \sigma_j^6 \quad (16-17)$$

Success in researching the existence of relationships (9), (10), (14) and (15) in turbulent bounded flows was the motive for other researches to perform similar analysis in the free flows. The first was *Matović*, who used single-component laser-Doppler anemometer in order to test the connections (9) and (10) in the free round jet [11]. His experimental data suffered from a convergence problem, caused by very short sampling time-interval. However, even within dispersed resulting data, mentioned relationships were still visible.

Results of *Matović*, together with [5], motivated *Petrović* to perform similar experiment in the free round jet [15]. He applied X hot-wire probe for measurement of the velocity moments up to the sixth order and verified relationships (9), (10), (14) and (15). The same reference also contains a comprehensive database of turbulent free round jet statistics. Improved analysis of these data is presented in [16].

According to reviewed data, we believed that both bounded and free turbulent flows follow the same, or at least very similar, relationships between higher-order correlations of fluctuating velocity components. In order to prove it, detailed measurement of turbulent velocity field of the plain wake behind a round cylinder was performed. Special attention was paid to connections based on the Gram-Charlier series expansions. Although they are self-consistent with the structure of time-averaged Navier-Stokes equations, it is always necessary to define an applicability domain. The reason is their weak convergence in some situations, as it was shown in [13]. Furthermore, *Frenkiel and Klebanoff* reported that truncations of Gram-Charlier expansions could lead sometimes to negative values for some sections of the resulting probability density distribution function [7]. Some other researchers did not observe such difficulty [6]. Properties of truncated Gram-Charlier approximations of marginal distributions, mentioned above, motivated authors to extensively research the applicability of different relationships for higher-order correlations, resulting from the various degrees of their truncations. *Durst, Jovanovic and Johanson* proved experimentally their applicability in the wall-bounded turbulent shear flows [6].

## 4. EXPERIMENTAL SET-UP AND ENVIRONMENTAL CONDITIONS

Reported experiments were performed after sunset or during cloudy days, what resulted in very stable temperatures of environmental air: their variations were in the limits of only  $\pm 1.0^\circ\text{C}$ . Those conditions, together with air-conditioning of the wind channel recirculation-flow, resulted in very small temperature changes, less than  $\pm 0.1^\circ\text{C}$  during measurements and within  $\pm 0.2^\circ\text{C}$  during hot-wire probes calibration. Thanks to suitable temperature conditions, temperature corrections for hot-wire anemometer readings were not necessary.

Turbulent plain wake was generated by a  $D=3\text{mm}$  cylinder, mounted in the working square cross-section (1.87m wide, 1.4m high and 2m long) of the large wind channel in the Lehrstuhl für Strömungsmechanik at the Friedrich-Alexander Universität Erlangen-Nürnberg. Free-stream mean velocity of 6.44m/s gave Reynolds number  $\text{Re}_D=1300$  (based on the cylinder diameter). Suitable design of the channel provided low free-stream turbulence level of only 0.07% for the streamwise direction and 0.04% in the normal and lateral direction of the flow. Measurements were performed in the cross-sections distanced 200, 300 and 400 rod diameters. Unfortunately, dimensions of the existing test-section didn't enable measurements at larger distances behind a cylinder, what was the only reason to exclude them from the research plan.

Three channels of the constant-temperature anemometer DISA M10 were employed together with two classic DANTEC hot-wire probes. Both, the X probe 55P61 and single-wire probe 55P11 possessed standard sensors with aspect ratio of 200 ( $L = 1\text{mm}$ ;  $d = 5\mu\text{m}$ ). They were applied simultaneously, in order to provide equivalent experimental conditions and check the validity of experimental data. Furthermore, possible influence of probe geometry (i.e. the influence of velocity gradients) was checked. Wires were operated at an overheat ratio of 0.6, which corresponds to the working temperature of  $\sim 250^\circ\text{C}$ .

The output anemometer voltages were processed by bucking-up amplifiers in order to increase the resolution of analogue-to-digital-conversion. In the exit stages of these amplifiers, signals were introduced in the built-in low-pass electronic filters of the fourth-order, with fixed cut-off frequency of 10kHz. Data were simultaneously sampled from the all three channels, at  $f = 3 \times 5\text{kHz}$ , using 16-bit DATA TRANSLATION ADC. At each measuring position, sampling time was set to 2 min. The auto-correlation function, calculated across the wake, gave an integral time-scale of the order of 0.002 sec (i.e. about 30 000 statistically independent data-points per each measuring position).

Cosine-law was used to describe hot-wires cooling in the case of X probe. Effective cooling angles  $\alpha_e$  were estimated following procedure of *Bradshaw* [1]. Both X and single-wire probes were calibrated in the free-stream part of the flow, against Pitot tube. Calibration data were fitted following [3]:

$$E^2 = B + K \cdot U_e^N \quad (18)$$

where  $E$  is the anemometer output voltage and  $U_e$  hot-wire effective cooling velocity, while  $B$ ,  $K$ , and  $N$  represent calibration constants. Although simple, expression (18) enabled high-precision measurement, thanks to favorable experimental conditions: mean velocities were high enough (over the "critical" range between 0 and 5m/s), their changes in the profiles were smaller than 0.5m/s and turbulence levels were low (below 2% in all three measuring cross-sections).

## 5. VERIFICATION OF THE TECHNIQUE

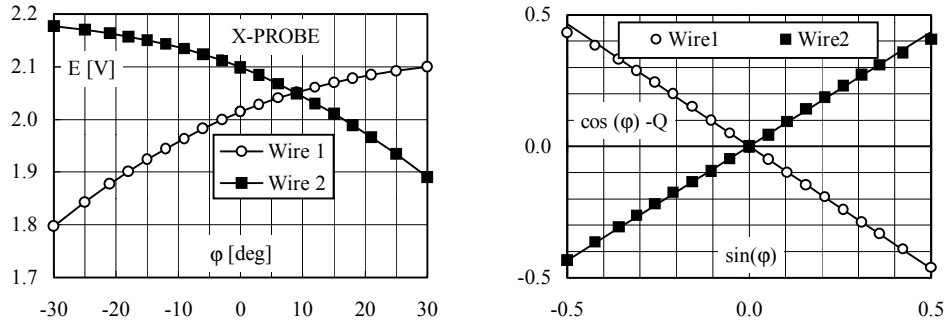


Fig. 1. (left) Pitch-calibration voltages of the sensors of X probe DANTEC 55P61.

Fig. 2 (right) Illustration of Bradshaw's [1] procedure for wires effective cooling angles evaluation.

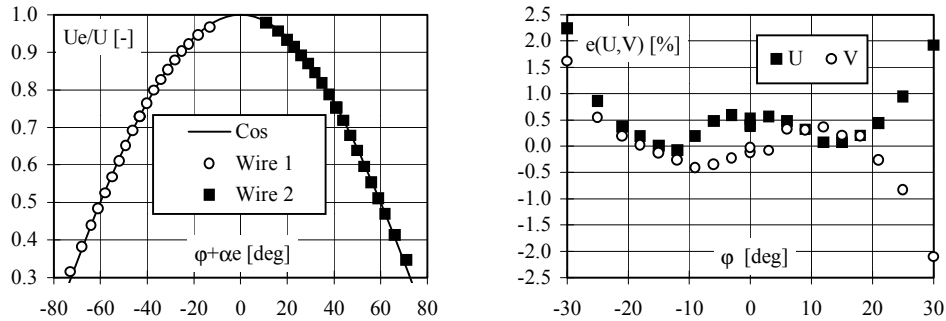


Fig. 3. (left) Deviations of the calibration data from the cosine law.

Fig. 4. (right) Reproduction errors of the induced streamwise and normal velocity components.

In order to test the validity of the applied cosine law, for DANTEC 55P61 X probe, the pitch calibration of the probe was performed in the wide angular range of  $\pm 30^\circ$ . Corresponding calibration voltages, presented in fig. 1, are used for numerical reproduction of the induced  $U$  and  $V$  fluid velocity components. Procedure of Bradshaw [1] for evaluation of effective hot-wire cooling angles is illustrated in fig. 2, where  $Q$  designates:

$$Q = \sqrt{(E(\varphi)^2 - E_0^2) / (E(\varphi=0)^2 - E_0^2)} \quad (19)$$

As can be seen in fig. 2, experimental data follow the straight lines very well, up to  $25^\circ$ . Fig. 3 additionally confirms the same statement: hot-wire cooling mechanism follows the cosine law in the same range of attack angles of fluid velocity vector toward the probe axis ( $U_e$  denotes effective cooling velocity and  $U$  is induced calibration velocity). Finally, full verification of the applied algorithm can be found in fig. 4: reproduction errors of the streamwise  $U$  and normal  $V$  velocity components are below 1% for pitch angles within the range of  $\pm 25^\circ$ .

## 6. MEAN TURBULENCE STATISTICS IN THE PLAIN WAKE BEHIND A CYLINDER

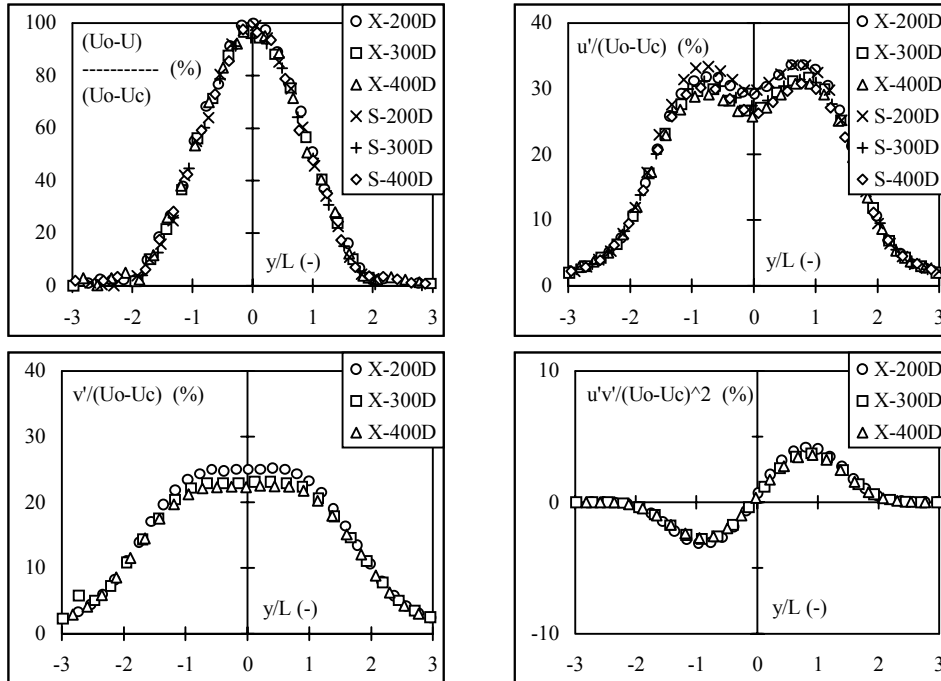


Fig. 5. Non-dimensional profiles of the mean velocity and Reynolds-stress components.

Results of measurement of the mean velocity component  $U$ , longitudinal  $u'$  and transversal  $v'$  turbulence intensity and Reynolds shear stress  $u'v'$ , by X-wire (X) and single-wire (S) probe, are presented in fig. 5. All three profiles, distanced 200, 300 and 400 diameters (D) downstream the rod, are (as usual) normalized by the mean fluid velocity deficit  $(U_c - U_0)$ , expressed as a difference between the mean free stream  $U_0$  and mean wake-center velocity  $U_c$ . In the same figure, abscissa corresponds to non-dimensional transversal coordinate  $y/L$ , normalized by distance  $L$  from the wake axis where the mean fluid velocity deficit is equal to one half of deficit of the wake center-mean-velocity  $U_c$ .

Profiles of skewness  $S$ , flatness  $F$ , superskewness  $SS$  and superflatness  $SF$  factors of the probability density distributions, for  $U$  and  $V$  velocity components, are illustrated in figs. 6, 7, 8 and 9. Figs 6 and 7 clearly show that profiles of central moments up to the fourth order are self-similar, when drawn toward non-dimensional wake width  $y/L$ . However, profiles of  $SS$  and  $SF$  are self-similar only in the inner region of the flow, approximately for  $|y/L| < 2$ , while the outer part of the wake is still not developed completely.

This behaviour of higher-order moments is wellknown in turbulence experimental practice. In other words, they need larger distance downstream the cylinder to achieve self-similarity in comparison to mean velocity and lower order correlations. However, it should be noted that achieving self-similarity of higher-order velocity correlations,

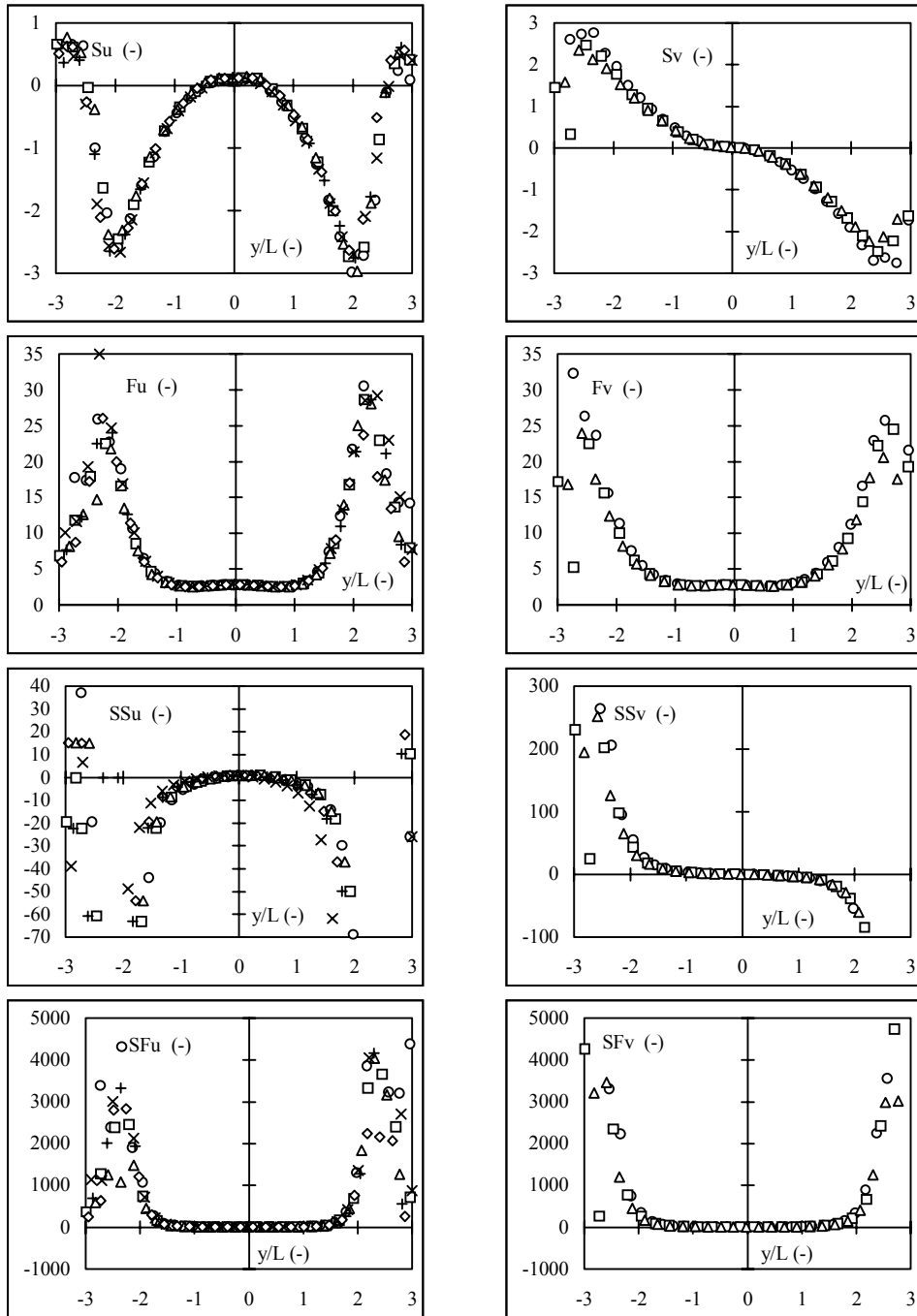


Fig. 6-9. Profiles of the non-dimensional velocity moments in the turbulent plain wake behind a round cylinder.

at distances below  $500D$ , are fairly rare in the wake flows (see [18]). Although we didn't check it explicitly, this phenomenon should be connected with the influence of initial conditions [8,9].

It should be noted that small asymmetry between the left and right side of the profiles is evident. Still, it is in acceptable limits that are present in nearly all experiments of this kind. For example, similar behavior of non-dimensional profiles can be found in [20].

#### 7. VERIFICATION OF THE RELATIONSHIPS BETWEEN HIGHER ORDER MOMENTS IN THE TURBULENT PLAIN WAKE BEHIND A CYLINDER

The goal of present study was to check the existency of statistical relationships between higher-order moments of the probability density distributions of turbulent velocity components. Corresponding results are illustrated in figs. 10, 11, 12 and 13.

In general, skewness  $\mathbf{S}$  and flatness  $\mathbf{F}$  factors (measured in the wake) fairly well follow the formulas (9) and (10), previously proved in the boundary layer and free round jet. However, data are slightly more dispersed around them, especially in the case of longitudinal  $\mathbf{U}$  velocity component and in the outer part of the wake (at  $|y/L| > 2$ ). The asymmetry around ordinate axis of the relationships between longitudinal skewness and flatness factors is quite logical, if one have on mind the structure of the wake flow (see [14] for example). In opposite, as it was expected, the shape of corresponding relationship for transversal  $\mathbf{V}$  velocity component is symmetric around the same axis. It is amazing that three crucially different flow configurations (boundary layer, jet and wake) follow nearly the same lines (9) and (10). This conclusion is in full agreement with expectation of [5] and [4].

Relationships between even and odd central moments  $\mathbf{SS} = \mathbf{f}(\mathbf{S})$  and  $\mathbf{SF} = \mathbf{f}(\mathbf{F})$  are also tested toward corresponding formulas (14) and (15), based on the truncated Gram-Charlier series expansions. As can be seen in fig. 11, connection  $\mathbf{SS} = \mathbf{f}(\mathbf{S})$  exists in the wake flow. Data are highly concentrated around lines  $\mathbf{SS} = 10\mathbf{S}$  in the inner region  $|y/L| < 1.5$ . However, it seems that skewness and superskewness factors are related around the curves that corresponds to cubic parabolas.

In the case of even moments  $\mathbf{SF}$  and  $\mathbf{F}$ , situation is slightly better (see fig. 12). Our experimental data follow line (15) in slightly wider range, up to  $|y/L| < 1.75$ . But, from the current level of our knowledge, it seems that second order regression parabola should be generally used for describing these relationships. Also, it is evident that larger data dispersion corresponds to longitudinal component  $\mathbf{U}$ , in comparison to transversal  $\mathbf{V}$  fluid velocity.

The relationships between superflatness  $\mathbf{SF}$  and superskewness  $\mathbf{SS}$  factors are presented in fig. 13, toward lines:

$$SF_U \approx 9.75 + 0.243SS_U^2 \quad SF_V \approx 16.95 + 0.372SS_V^2 \quad (20-21)$$

derived by combining (9) with (14) and (10) with (15), respectively. Existence of the relationships between superflatness and superskewness factors is evident in that figure. However, the experimental data weekly follow lines (20) and (21). In general, agreement is excellent only near the values that correspond to Gaussian probability density distribution. Dispersion of experimental data around the general trend lines is present much more in the case of  $\mathbf{U}$  component, in comparison to  $\mathbf{V}$ .

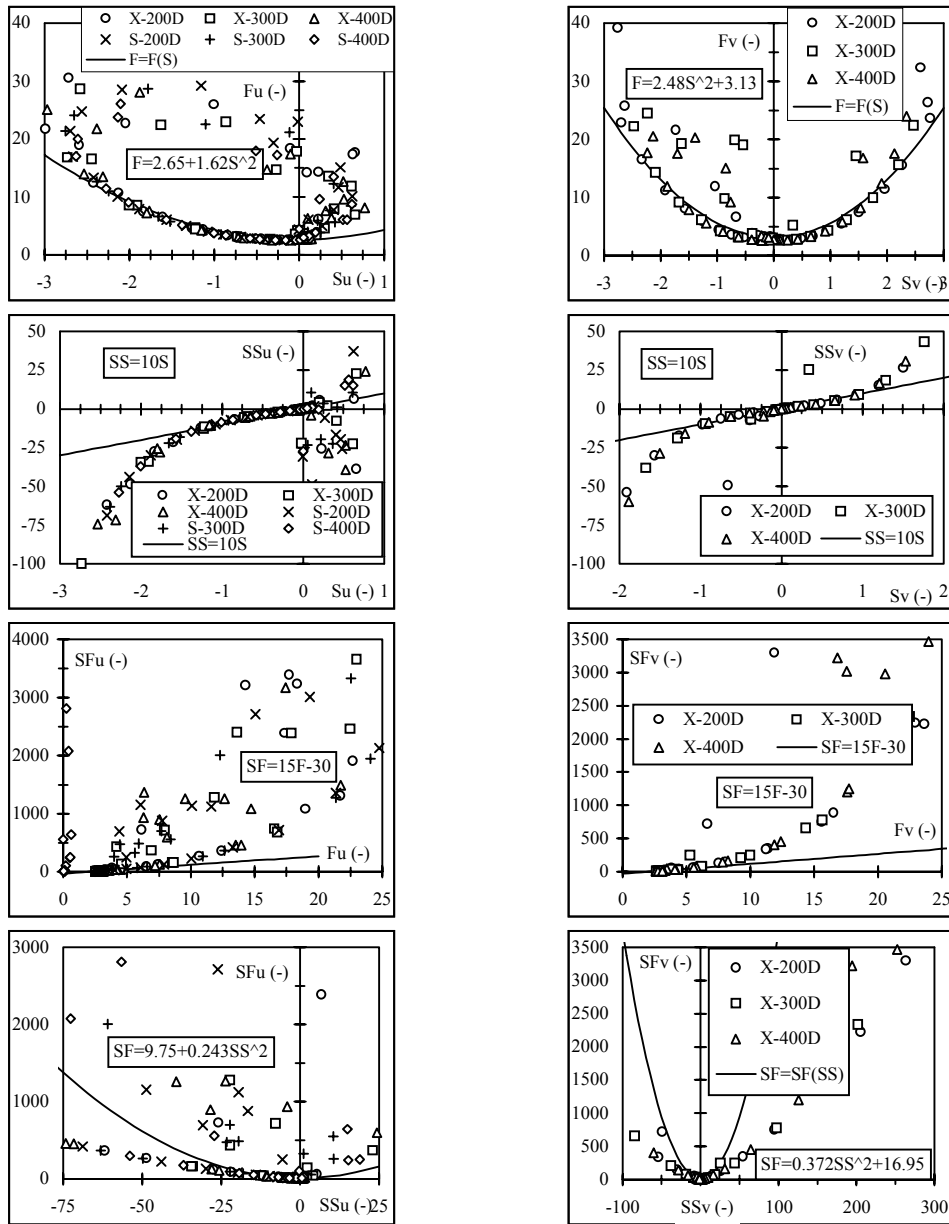


Fig. 10-13. Velocity correlations in the turbulent plain wake behind a round cylinder.

At the end of this chapter, it should be noted that agreement between data measured by DANTEC X probe (55P61) and single-wire probe (55P11) is nearly perfect, what means that the influence of probe geometry was negligible in our experiment. Although turbulence level was extremely low in tested flow, this result is important. Our intention

was to ensure high measurement precision, because [17] and [19] evidenced strong influence of hot-wire probes configuration on the measurement results of higher-order correlations of the turbulent velocity field. Furthermore, we checked Kolmogorov microscale. It was smaller than 0.5mm, providing fine spatial resolution for both applied hot-wire probes.

#### 8. AN ADDITIONAL TEST AT LARGE REYNOLDS NUMBER

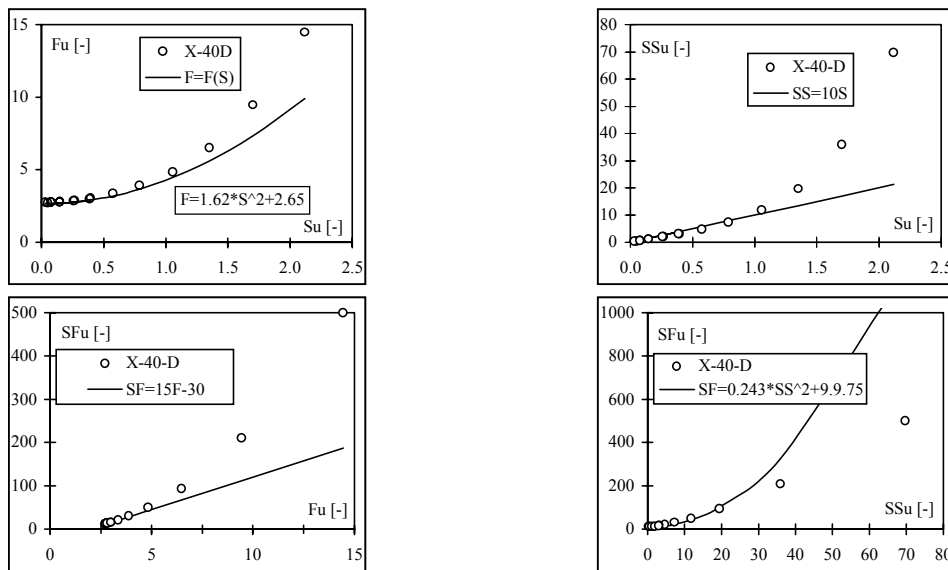


Fig. 14-17. Velocity correlations in the near field of the turbulent plain wake behind a round  $D=50\text{mm}$  cylinder.

After analysis presented in the chapter no. 7, a following question (among many others) arise: “Isn’t it possible that deviations of the experimental data, from the trend lines (14), (15), (20) and (21) could be initiated by the influence of low-Reynolds number”? In order to check this possibility, an additional preliminary experiment was performed in the near-field of the plain wake behind a  $D = 50\text{mm}$  cylinder. Measuring cross-section was positioned 2000mm (40D) downstream the cylinder. The mean velocity of the free-stream flow was increased to 32m/s, providing quite a huge Reynolds number of  $Re_p = 108000$ . However, turbulence levels in the measuring cross-section of the wake were still moderate, below  $\sim 9\%$ , permitting successful application of X-wire probe. Moreover, this additional analysis is improved by providing the large amount of 240000 statistically significant data, hoping that they will decrease uncertainty of the experimental data (scatter).

Having on mind the limitations of printing space and the auxiliary purpose of the second experiment, corresponding results are presented only partially in figs. (14-17). They generally confirm the results of the first experiment, performed at low-Reynolds number in the wake far-field: relationships between higher-order velocity moments are

verified, but they don't follow quite exactly the trend lines evidenced in the turbulent boundary layer and free jet. As it was expected, data-scatter is significantly decreased in the second experiment in comparison to the first. This was achieved thanks to increased number of statistically significant data samples.

## 9. CONCLUSIONS

In the present study are verified the statistical relationships between the skewness  $S$  and flatness  $F$  factors of the streamwise and cross-stream velocity components in the plain wake behind a round cylinder. They are practically identical to corresponding relationships noticed in the turbulent boundary layer [4] and free round jet [16].

However, this situation is different in the case with relationships based on the truncated Gram-Charlier series expansions:  $SS = 10S$  and  $SF = 15F - 30$ . The skewness and superskewness factors follows line  $SS = 10S$  fairly well only in the inner region of the wake, limited approximately by  $|y/L| < 1.5$ . Similarly, relationships  $SF = f(F)$  can be described by  $SF = 15F - 30$  only in the inner wake region:  $|y/L| < 1.75$ .

Analysis of the connections  $SF = f(SS)$  shows that some trends also exist. However, the lines (20) and (21) does not describe the real situation accurately. The only exception of this statement is evidenced just in the very narrow region around the wake axis, where corresponding velocity distributions are close to Gaussian. Although experimental data are dispersed around the main statistical trends, especially in the case of longitudinal velocity component, they are still highly concentrated around them.

The agreement of data measured by  $X$  and single-wire probe is excellent, showing that the influence of probe geometry on the measurement results is negligible. Furthermore, two experiments performed at various Reynolds numbers gave generally similar results. Follows that the influence of Reynolds number is not a reason for deviations of our experimental data from the trend-lines previously evidenced in the boundary layer.

Discussed deviations are slightly surprising, having on mind that *Petrović* proved the validity of relationships (9), (10), (14), (15), (20) and (21) in the round jet that is also boundary-free flow such as wake [15]. However, one must have on mind that small deviations of the experimental data of [15] from these lines are reported in [16]. Possibly wrong, but they were explained as direct consequences of measuring errors at low fluid velocities in the outer region of the jet. In the wake, it would not be a correct explanation, because the mean free-stream velocity, which corresponds to the wake outer zones, was not low. Its magnitude was above 6m/s in the first, and even greater than 30m/s in the second experiment. Both velocity ranges are suitable for high-precision measurement by hot-wire anemometer.

At present, the reliable reason for the above-mentioned behaviour of wake statistics is still unknown and will be the subject of future investigations. However, we believe that it is caused by large deviations of the probability density distributions of turbulent velocity components (also evidenced here) from the normal. In such situation, expressions (11-13) and (16-17) for higher-order moments could be inappropriate, because they are formulated for the normal Gaussian distribution. Therefore, it is logical to expect that errors in moments evaluation by formulas (11-13) and (16-17) are increased in the wake, where the real distributions of fluid velocity components are far from the normal. These

evaluation errors could be a fairly reliable explanation for deviations of our results from the analogue trends in the boundary layer. Our belief is additionally supported by verification that influences of probe geometry and low Reynolds number were negligible in this case.

It can be concluded that large variations of higher-order moments around Gaussian values make the wake-flow configuration statistically more complex in comparison to free jet and bounded flows. However, our data show that both free and bounded turbulence still follow similar statistical relationships.

We believe that a new experiment in the wake would be needed in the nearest future. It should be performed at various Reynolds numbers, within the wider range of distances of measuring cross-sections. In the region close to the cylinder, the more sophisticated probe with four hot-wires should be applied, in order to enable high measurement accuracy for all three velocity components and wide uniqueness cone (see [14]). These data could be analyzed following [5], who reported the applicability of general distribution function for describing the probability density distribution of turbulent velocity components through the whole boundary layer. In that case, expressions (11-13) and (16-17) for evaluation of higher-order moments should be exchanged by new adequate formulas for the general distribution function [5].

#### REFERENCES

1. Bradshaw P. (1971): *An introduction to turbulence and its measurement*, Pergamon Press, Oxford, New York, Toronto, Sydney, Braunschweig.
2. Coles E. D. (1962), *The turbulent boundary layer in compressible fluid. Appendix A: A manual of experimental practice for low speed flow*, Random Report R403R-PR, ARC24473.
3. Davies P. and Bruun H. H. (1969), *The performance of yawed hot wire*, ISVR report no. 284.
4. Durst F. and Jovanović J. (1995), *Investigations of Reynolds-averaged turbulence quantities*, Proceedings of Royal Society London A(1995) 451, p. 105-120.
5. Durst F., Jovanović J. and Kanevče Lj. (1987), *Probability density distribution in turbulent wall-bounded shear layer flows*, Turbulent Shear Flows, Springer-Verlag 5, p. 197-220.
6. Durst F., Jovanović J. and Johanson T. G (1992), *On the statistical properties of truncated Gram-Chalier series expansions*, Journal of Physics of Fluids, A4(1), p. 118-126.
7. Frenkiel N. F. and Klebanoff S. P. (1967), *Higher-Order Correlations in a Turbulent Field*, Journal of Physics of Fluids, vol. 10, no. 3, p. 507-520.
8. Hussain A. K. M. F. and Zedan F. (1978), *Effect of the initial conditions on the axisymmetric free shear layer: Effect of the initial fluctuation level*, Journal of Physics of Fluids, vol. 21 no. 7, p. 1100-1112.
9. Hussain A. K. M. F. and Zedan F. (1978), *Effect of the initial conditions on the axisymmetric free shear layer: Effect of the initial momentum thickness*, Journal of Physics of Fluids, vol. 21 no. 9, p. 1475-1481.
10. Jovanović J., Durst F. and Johanson T. G. (1993), *Statistical analysis of the dynamic equations for higher-order moments in turbulent wall-bounded flows*, Journal of Physics of Fluids, A5(1), p. 2886-2900.
11. Matović M. (1998), *Experimental investigation of free premixed flame flow field, by laser anemometer*, Master thesis, University of Belgrade, Faculty of Mechanical Engineering in Belgrade, (in Serbian).
12. Moin P. (1992), *The computation of turbulence*, Aerospace America, no. 1, p. 42-46.
13. Monin A. S. and Jaglom A. M. (1975), *Statistical Fluid Mechanics*, The MIT Press, Cambridge, Massachusetts and London, UK.
14. Ong L. & Wallace J. (1996), *The velocity field of the turbulent wake of a circular cylinder*, Experiments in Fluids, no. 20, p. 441-453.
15. Petrović V. D. (1991), *Research of turbulent fluid flow in the free round isothermal jet by hot wire anemometer*, Master thesis, University of Belgrade, Faculty of Mechanical Engineering, (in Serbian).
16. Petrović V. D., Benisek M. and Oka N. S. (1997), *Statistical relationships in a turbulent free round jet*, Proceedings of the Second International Symposium on Turbulence, Heat and Mass Transfer, Delft University Press, Delft, The Netherlands, p. 173-179.

17. Vukoslavčević V. P. and Wallace M. J. (1996), *A twelve-sensor hot wire probe to measure the velocity and vorticity vectors in turbulent flow*, Measuring Science and Technology, vol. 7, p. 1451-1461.
18. Tennekes H. and Lumley L. J. (1978), *A first course in turbulence*, The MIT Press, Cambridge, Massachusetts and London, UK.
19. Vukoslavčević V. P. and Petrović V. D. (1997), *Influence of hot-wire probe configuration on the results of 3-d fluid velocity field measurements*, Proceedings of the Second International Symposium on Turbulence, Heat and Mass Transfer, Delft University Press, Delft, The Netherlands, p. 189-199.
20. Qiao-yan Ye (1996), *Die turbulente dissipation mechanischer energie in scherschichten*, Ph. D. thesis, Lehrstuhl für Strömungsmechanik, Technische Fakultät Friedrich-Alexander Universität Erlangen-Nürnberg.

**Acknowledgments:** *The support of the Deutscher Akademischer Austauschdienst DAAD (two-month study visit to LSTM Erlangen of D. Petrović - ref. ub-324/97) and Ministry of Science and Technology of Republic of Serbia (project 08M01) is gratefully acknowledged. The authors are also grateful to Dr. J. Jovanović and Mr. H. Lienhart for providing advice and encouragement.*

## KORELACIJE BRZINE U TRAGU IZA CILINDRA

**Dragan V. Petrović, Thoralf C. Schenck, Franz Durst**

*U radu je potvrđeno postojanje statističkih veza visih momenata brzine u dalekom polju ravanskog traga iza cilindra. Mada su izvesne razlike prisutne, ove veze su analogne opstim trendovima prethodno uocnim u turbulentnom granicnom sloju i slobodnoisticucem mlazu:  $SS_{u,v}=10*S_{u,v}$ ,  $SF_{u,v}=15*F_{u,v}-30$ ,  $F_u=1.62*S_u^2+2.65$  and  $F_v=3.13*S_v^2+3.48$ . One predstavljaju dobru osnovu za dalje statističke analize turbulentnih tokova i resavanje problema zatvaranja sistema karakteristiknih jednacina strujanja.*